

Electric potential patterns in the northern and southern polar regions parameterized by the interplanetary magnetic field

V. O. Papitashvili,¹ B. A. Belov, D. S. Faermark, Ya. I. Feldstein, S. A. Golyshev, L. I. Gromova, and A. E. Levitin

Institute of Terrestrial Magnetism, Ionosphere, and Radio Wave Propagation, Troitsk, Moscow Region, Russia

Abstract. Electric potential patterns have been obtained from the IZMIRAN electrodynamic model (IZMEM) for the northern and southern polar regions during summer, winter, and equinox. The model is derived from a large quantity of high-latitude ground-based geomagnetic data (above $\pm 57^\circ$ corrected geomagnetic latitude) at all magnetic local time hours. A linear regression analysis technique has been used to obtain the quantitative response of each magnetic observatory to changes of interplanetary magnetic field (IMF) components. Since no ionospheric conductivity model exists specifically for the southern polar region, the statistical model of Wallis and Budzinski (1981) has been applied in both hemispheres. A cross-polar “background” potential of ~ 35 kV, derived by Reiff et al. (1981), is used to calibrate IZMEM’s potential patterns. The model’s responses to changes in the IMF B_y and B_z components are analyzed to obtain a set of “elementary” convection patterns in both polar regions for each season of the year. Asymmetry in the potential pattern geometry in both hemispheres can be attributed either to the influence of the “northern” ionospheric conductivity model which was applied to the southern polar region, or to some natural phenomena. The modeled background cross-polar potential for the condition when $B_z = B_y = 0$ is found to be ~ 37 kV. Average values of the modeled potential drop caused by each nanotesla of the IMF are the following: ~ 14 kV for southward B_z ; ~ -4 kV for northward B_z ; and $\sim \pm 4.5$ kV for B_y components. The latter is not applicable to the “dawn-dusk” potential drop; it may be applied across the cusp region only. Nevertheless, a combination of the background and elementary potential patterns in the case studies gives a certain estimation of the cross-polar potential drop, which may be strongly distorted during time of large B_y . It is concluded that IZMEM provides realistic convection patterns parameterized by the IMF component directions and magnitudes and may be used to provide routine estimates of convection patterns and electric potentials if IMF data are available.

Introduction

Interpretation of ground-based geomagnetic perturbations by means of ionospheric electric fields and currents began with the fundamental works of K. Birke-land, S. Chapman, and H. Alfvén. Since then Kern [1966] found a relation between the scalar current function obtained from divergence-free portion of the steady current distribution in a thin spherical layer and the density of the field-aligned currents in the case of a uniform ionospheric conductivity. Because of the nonuni-

form character of ionospheric conductivity, novel numerical methods have been developed to resolve the equations that relate the magnetic field perturbations on the Earth’s surface to the ionospheric electric field potential [Faermark, 1977; Mishin et al., 1980; Kamide et al., 1981]. The evolution of ideas set forth by Chapman and Alfvén has been presented in detail by Feldstein and Levitin [1986]. Considerable progress has been made since that time in inferring three-dimensional current systems by combining the ground-based magnetic data and modeled ionospheric electric potential and fields. The assimilative mapping of ionospheric electrodynamics (AMIE) technique [Richmond and Kamide, 1988], which is a further development of the KRM method [Kamide et al., 1981], has begun to be widely used for the analysis of electrodynamic state of the high-latitude ionosphere [e.g., Knipp et al., 1991].

Empirical models of high-latitude electric fields for different orientations of the IMF have been developed

¹Also at Space Physics Research Laboratory, University of Michigan, Ann Arbor, Michigan.

from satellite observations [e.g., *Heppner, 1977; Heppner and Maynard, 1987; Hairston and Heelis, 1990*]. Subsequent synoptic studies of radar measurements [see *Foster, 1983; Alcayde et al., 1986; de la Beaujardiere et al., 1991*] have yielded results that are in substantial agreement with statistical satellite models. Most of the ground-based magnetometer studies that are based on the KRM and later the AMIE techniques also show a good agreement with satellite and radar models [e.g., *Friis-Christensen et al., 1985; Knipp et al., 1993*]. There are also a number of reports representing the theoretical approaches to the modeling of high-latitude convection patterns [see *Heelis et al., 1982; Clauer and Friis-Christensen, 1988; Blomberg and Marklund, 1991*, and references therein].

At the end of the 1970s, numerical techniques which are similar to the KRM were developed independently by two scientific groups in Russia: the IZMIRAN electrodynamic model (IZMEM) at the Institute of Terrestrial Magnetism, Ionosphere, and Radio Wave Propagation, Troitsk, Moscow Region [*Belov et al., 1977*], and the technique of inversion of the magnetograms (TIM) at SibIZMIR, Irkutsk [*Mishin et al., 1977*]. We refer the reader to the original work of *Mishin et al.* [1980] for details of the TIM technique. Here we shall describe the IZMEM method only.

AMIE, KRM, and TIM techniques analyze ground-based magnetic field perturbations derived for an event with a duration from a few hours to a few days. They require a selection of nearby "magnetically quiet" period which is a most subjective part of the analyses because the IMF conditions might be considerably different for "disturbed" and "quiet" periods. These techniques use also spherical harmonic expansion to process initial geomagnetic data and cover sizable gaps between magnetic observatories, especially at high latitudes. Therefore the expansion uncertainties are much higher, for example, in the Arctic ocean or Antarctic region than for Canada or Scandinavia.

At IZMIRAN, a regression analysis was used to study geomagnetic variations caused by changes in the interplanetary magnetic field (IMF). Initial results have been published in Russian in the proceedings of IZMIRAN and *Geomagnetism and Aeronomy* [e.g., *Afonina et al., 1980*] (see other references in the work by *Levitin et al.* [1982] and *Feldstein et al.* [1984]). These investigations have utilized geomagnetic data from the northern polar region only. However, using magnetic observations from the southern polar cap [*Mansurov et al., 1981*], we have applied the same regression technique to the Antarctic data [*Papitashvili et al., 1983, 1989, 1990*]. This approach provides a parameterization of geomagnetic variations by the IMF, and the ionospheric electrodynamics may then be defined. The IZMEM does not require a selection of magnetically quiet period or use of the spherical harmonic expansion. These distinguish the IZMEM from other techniques.

The purpose of this paper is to describe briefly a numerical scheme of the IZMEM, present a summary of results obtained in the form of average patterns of

the high-latitude electric potential in both hemispheres parameterized by the IMF conditions, and show the IZMEM's ability to model electric potential patterns for any moment of time when the IMF data are available. The numerical scheme also estimates ionospheric electric fields associated with three-dimensional current systems. The model has a transportable FORTRAN code and may be run on a personal computer.

Model Description

We postulate that the magnetosphere-ionosphere coupling link can be considered as a black box, which accepts changes of the IMF and solar wind plasma (SW) parameters (B_x , B_y , B_z , velocity V , and density n) as an input signal, and induces ground-based geomagnetic perturbations as an output signal. This approach has already been used in others works, in particular, those employing the linear prediction analysis [see *Clauer, 1986*, and references therein]. A number of interplanetary parameters are known to be associated with magnetospheric interaction [*Levitin et al., 1982*]. For example, there is much evidence in the literature showing impact of the IMF B_y and B_z components on the magnetic field at the Earth's surface. The division of B_z into negative and positive values may represent disturbed and quiet geomagnetic conditions, respectively, though a northward B_z can induce a strong polar cap currents as well. The IMF B_x component has been found to show little correlation with geomagnetic variations [*Maezawa, 1976; Levitin et al., 1982; Troshichev, 1982*]. Therefore we can compute the regression coefficients K_{B_x} but may disregard their contribution to the model. We have tried a number of SW parameters (velocity V , density n , temperature T , and some of their combinations) to find a better correlation with ground-based data and concluded that V^2 and nV^2 show significant correlations. The V^2 term may, in part, represent "quasi-viscous" interaction of the solar wind plasma with Earth's magnetosphere; the nV^2 is proportional to dynamic pressure of the solar wind.

We use a regression model where regression coefficients relate any ground-based geomagnetic field component, for example, H , to changes of the corresponding IMF parameter:

$$H^i = K_{HB_x}^i B_x^i + K_{HB_y}^i B_y^i + K_{HB_z}^i B_z^i + H0^i \quad (1)$$

The free term of equation (1) can be expanded for the solar wind parameters:

$$H0^i = K_{HV^2}^i V_i^2 + K_{HnV^2}^i n_i V_i^2 + H00^i \quad (2)$$

Here K_H^i are regression coefficients for $i = 1, \dots, 24$, where i is universal time (UT) hour; $H0^i$ is a residual part of (1) for the average conditions of solar wind ($n = 4 \text{ cm}^{-3}$, $V = 450 \text{ km/s}$); $H00^i$ represents geomagnetic variations which are free of the IMF and SW impact (we shall omit index i further). In this paper we shall consider the model parameterized by the IMF

only and refer the reader to the work by *Levitin et al.* [1982] and *Papitashvili et al.* [1990] where the solar wind parameters are considered.

The total hourly mean values of the IMF and ground-based geomagnetic data for each season of the year (summer, winter, and equinox) and both northern and southern polar regions above $\varphi = \pm 57^\circ$ corrected geomagnetic (CGM) latitude have been used in the regression analyses. The regression geomagnetic model for the northern polar region has been developed using the data from 15 magnetic observatories in 1968–1969 [*Levitin et al.*, 1982]. The northernmost station was Thule ($\varphi = 86.2^\circ$). The same model for the southern hemisphere has been obtained from the 1978–1980 and 1983–1984 data (21 magnetic observatories and autonomous magnetometers). Here the data from four stations poleward of -85° latitude were available and the southernmost station was at $\varphi = -89.1^\circ$ [*Papitashvili et al.*, 1990].

The arrays of the IMF and geomagnetic data were subjected to regression analyses for each of 24 UT hours of each day over the entire season of the year (120 days). The resultant magnetic local time (MLT) daily variation of regression coefficients K_H and ΔH_0 around daily mean value $\overline{H_0}$ were obtained. These results have been compared for the same hourly mean values of the IMF and geomagnetic data, and IMF values one hour

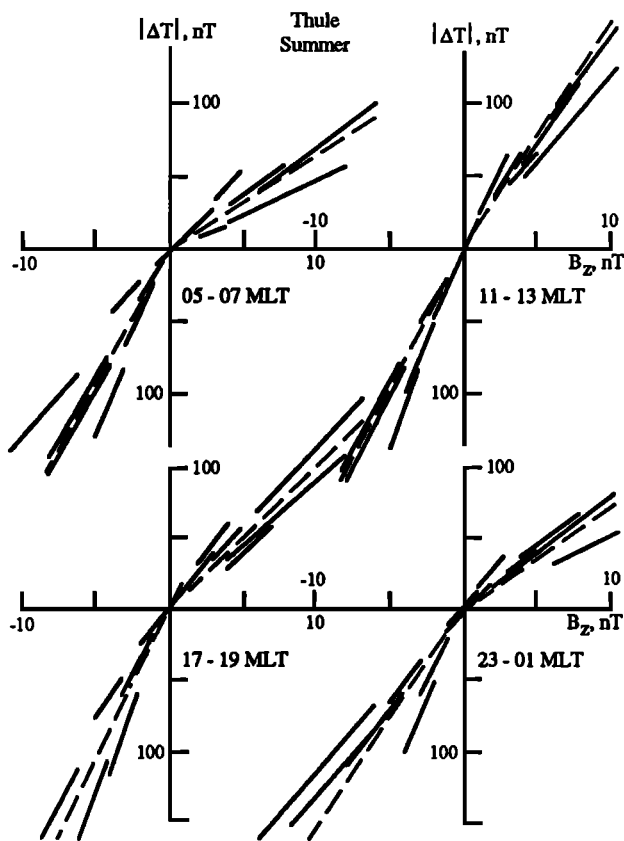


Figure 1. Linear regression dependence of an intensity of geomagnetic field horizontal component perturbation at Thule against the negative and positive IMF B_z values. [After *Papitashvili et al.*, 1981].

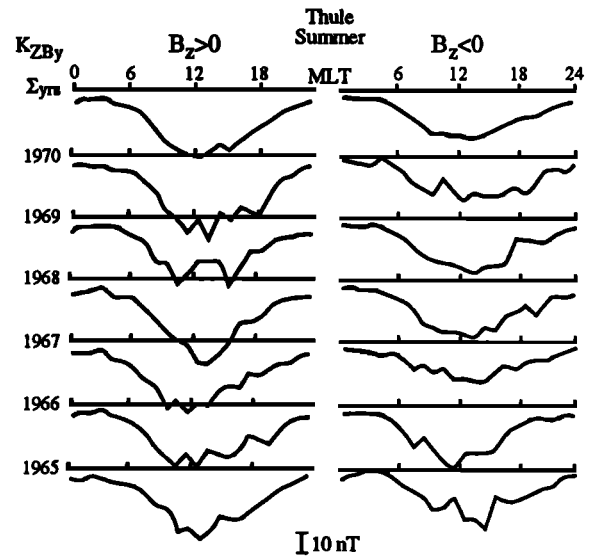


Figure 2. Diurnal variation of K_{ZB_y} regression coefficient at Thule during 1965–1970. [After *Papitashvili*, 1982].

ahead of the ground-based data. A better correlation was obtained when the same hourly mean values were compared.

With this model we assume that ground-based geomagnetic disturbances are proportional to variations of the IMF components and there are a variety of physical mechanisms that provide links that transfer energy from the solar wind plasma to the high-latitude magnetosphere and ionosphere. The assumed linearity was studied and confirmed for the B_z component [*Papitashvili et al.*, 1981; *Troshichev*, 1982]. Figure 1, for example, shows a dependence of the total horizontal component perturbation, $\Delta T = (K_{XB_z}^2 + K_{YB_z}^2)^{1/2}$, at Thule for negative and positive IMF B_z and for different MLT hours during summer. Dashed lines show a regression between ΔT and B_z for two separate arrays of original data: for $B_z < 0$, and $B_z > 0$. Short segments represent a regression between ground-based data and the IMF within binned (by 2–6 nT) intervals of B_z . All of these segments follow the corresponding dashed regression lines.

The solar cycle variation has been studied by *Papitashvili* [1982]. Figure 2 shows an example of the K_{ZB_y} diurnal variations for the Z component at Thule during the summer for each year separately (1965–1970), and for all of the original data combined into one array corrected for the secular variation. The magnitude and shape of the variations are similar for each year. Therefore a regression model of geomagnetic variations can be used over the entire solar activity cycle. These two studies (linearity and solar cycle) have been carried out for the polar cap stations only (Thule, Godhavn, Vostok, and Mirny), and they should be extended in future for the auroral and subauroral magnetic observatories.

The “regression modeling” approach has several advantages: (1) total values of geomagnetic field components are used in the analysis, and there is no subjective

selection of a perturbation baseline; (2) the technique uses many measurements made by a limited amount of magnetic observatories at different local times due to the Earth's rotation, therefore, 24 values of K_H are found for each observatory; (3) only an interpolation of K_H along meridians is required, instead of spherical harmonic expansion; (4) only the IMF values are required to model geomagnetic variations, and then electrodynamic parameters can be obtained using the IZMEM during all three seasons of the year in both northern and southern polar regions.

This regression model of geomagnetic variations is used as an input for numerical solution of the second-order partial differential equation [Faermark, 1977]:

$$\nabla \times (-\hat{\Sigma} \cdot \text{grad}\Phi) = \nabla \times [\mathbf{n}_r \times \text{grad}\Psi] \quad (3)$$

Here Φ is electrostatic potential ($\Phi = 0$ at $\varphi = \pm 57^\circ$), $\hat{\Sigma}$ is a tensor of nonuniform ionospheric conductivity, \mathbf{n}_r is a unit radial vector, and Ψ is an equivalent current function, uniquely related to geomagnetic perturbations on the Earth's surface. A definition of the current function in the IZMEM method is similar to that in the work by Kamide *et al.* [1981]. By analogy with the AMIE technique [Richmond and Kamide, 1988] the IZMEM approach represents a regression mapping of ionospheric electrodynamics (RMIE).

Equation (3) may be rewritten in spherical coordinates θ (colatitude) and λ (east longitude) [Feldstein and Levitin, 1986]:

$$\begin{aligned} & - \left[\frac{\partial}{\partial \theta} \left(\sin \theta \Sigma_H \frac{\partial \Phi}{\partial \theta} \right) + \frac{1}{\sin \theta} \frac{\partial}{\partial \lambda} \left(\Sigma_H \frac{\partial \Phi}{\partial \lambda} \right) \right] \\ & + \left[\frac{\partial}{\partial \theta} \left(\Sigma_P \frac{\partial \Phi}{\partial \lambda} \right) - \frac{\partial}{\partial \lambda} \left(\Sigma_P \frac{\partial \Phi}{\partial \theta} \right) \right] \\ & = \frac{\partial}{\partial \theta} \left(\sin \theta \frac{\partial \Psi}{\partial \theta} \right) + \frac{1}{\sin \theta} \frac{\partial^2 \Psi}{\partial \lambda^2} \end{aligned} \quad (4)$$

where Σ_H and Σ_P are height-integrated Hall and Pedersen ionospheric conductivities specified on a grid of 1° geomagnetic latitude and one MLT hour. Since no ionospheric conductivity models exist specifically for the southern polar region, the particle precipitation statistical conductivity model of Wallis and Budzinski [1981] and the solar UV conductivity model of Robinson and Vondrak [1984] are used for both hemispheres.

The distributions of electric potential can be determined and parameterized as a superposition of the IMF related terms:

$$\begin{aligned} \Phi(\varphi, \text{MLT}, B_z, B_y) &= \Phi_z(\varphi, \text{MLT}) A_{B_z} \\ &+ \Phi_y(\varphi, \text{MLT}) A_{B_y} + \Phi_0(\varphi, \text{MLT}) \end{aligned} \quad (5)$$

Here φ is a corrected geomagnetic latitude; MLT is magnetic local time; Φ may represent electric potential, as well as electric and magnetic fields, ionospheric (Hall and Pedersen) and field-aligned currents, or Joule heating rate; A_{B_z} and A_{B_y} are dimensionless amplitudes of

the IMF components for a given MLT hour; Φ_z and Φ_y are the solutions of (4) for each set of regression coefficients and correspond to changes of a given parameter (electric potential, ionospheric currents, etc.) on the IMF 1-nT step; Φ_0 is the solution of (4) for the sets of free term in (1) during different conditions in the IMF (e.g., negative or positive B_z and B_y).

The Φ_0 term in (5) represents the "background" potential, which exists in the ionosphere during average conditions in the solar wind, that is, "viscous" convection according to Reiff *et al.* [1981]. The other terms of the (5) represent the "elementary convection cells" at high latitudes caused by the IMF components. A combination of these elementary cells for definite conditions in the IMF will reproduce a typical convection pattern observed by satellites and radars over the polar regions. Therefore, as the (1) describes a basic structure of the high-latitude geomagnetic variations, the (5) allows one to construct a quantitative model of the ionospheric electrodynamics.

The IZMEM electrodynamic parameters have been obtained initially using the ionospheric conductivity distributions derived for 1700 UT and 0500 UT (north magnetic pole at local noon and midnight respectively). To avoid the UT dependence of the IZMEM output, the averaged ionospheric conductivity distribution (between two derived for 1700 UT and 0500 UT) has been used to compute the entire set of electrodynamic parameters. This averaging assumes that the geographic and geomagnetic poles are coincident. In this case the difference between the cross-polar potentials for the 'averaged' and UT-dependent models is about $\sim 25 - 30\%$, but the electric potential distributions are very similar. The following analysis and figures are presented for the UT-averaged model.

While we have used a commonly adopted division of the year into seasons (May–August: northern summer and southern winter, November–February: northern winter and southern summer; March, April, September, and October are equinoctial months for both hemispheres), it is also possible to bin the data by the Earth's dipole tilt and develop the UT-dependent model where the solar UV ionospheric conductivity will be better utilized.

Convection Patterns Parameterized by the IMF

The IZMEM model outputs (electric potential, electric and magnetic fields, ion convection velocity, etc.) have been already compared with the satellite and radar measurements [e.g., Belov *et al.*, 1984; Dremukhina *et al.*, 1985; Papitashvili and Clauer, 1993]. The calculated values of electrodynamic parameters are usually smaller than the measured data. Geomagnetic disturbances obtained from the regression model (1) have not been separated into the internal and external variations and extended upward on the ionospheric level. Therefore an amplification factor should be derived from the comparison with experimental data. For example, *Feld-*

stein and Levitin [1986] compared OGO 6 observations [Heppner, 1972] with the modeled electric fields and obtained the factor of 3.0. Another approach will be used to calculate amplification factors in this paper. (Note that all of the following figures present the uncorrected model outputs, that is, without the use of amplification factor.)

Modeled Electric Potential for $B_z = B_y = 0$

The ground-based geomagnetic data have been initially divided into two arrays according to the sign of B_z , that is, for the disturbed ($B_z < 0$) and quiet ($B_z > 0$) states of the magnetosphere. These arrays have been subjected to regression analyses separately. Therefore two sets of all terms in the equation (1) have been obtained. The free term in both cases shows geomagnetic disturbances remained in the polar regions when the IMF equals zero. The electric potential distributions inferred from the free terms should be similar for the disturbed and for the quiet conditions because the separate arrays are subsets from the general population.

Figure 3 shows electric potential distributions for the disturbed conditions. Similar distributions were obtained for the quiet conditions (not shown). These patterns may also be considered as "convection patterns" because ionospheric plasma moves along the equipotential lines: clockwise in the negative vortex and anti-

clockwise in the positive vortex. These particular patterns for $B_z = B_y = 0$ would be classified as viscous cells because the background potential "...remains when the merging theory predicts zero, and this residual may logically be attributed to non-merging (close model) transfer processes..." [Reiff et al., 1981, p. 7645].

The "standard" two-cell convection is well developed in both hemispheres; the vortices occupy almost the same areas for each season. There is a little asymmetry in the location of antisunward transpolar flows in both hemispheres, but they are directed generally from 0900–1000 MLT to 2100–2200 MLT. Reiff et al. [1981] have sketched the possible flow over the entire polar cap; however, Reiff and Burch [1985] have removed this flow for the zero IMF condition. We think that the convection flow across the center of polar cap may exist even when the IMF $B_z = B_y = 0$ because the magnetosphere will be closed completely and viscous interaction can take place over the entire magnetopause surface. For example, Friis-Christensen et al. [1985] have obtained the electric potential distribution for zero IMF, which is very similar to our "northern summer" pattern in Figure 3. It is particularly interesting how convection patterns are similar in both hemispheres, especially since they were obtained from the data of different years, and even different solar activity cycles.

Modeled cross-polar potential (the MAX-MIN value) shows a seasonal dependence. Averaged (between dis-

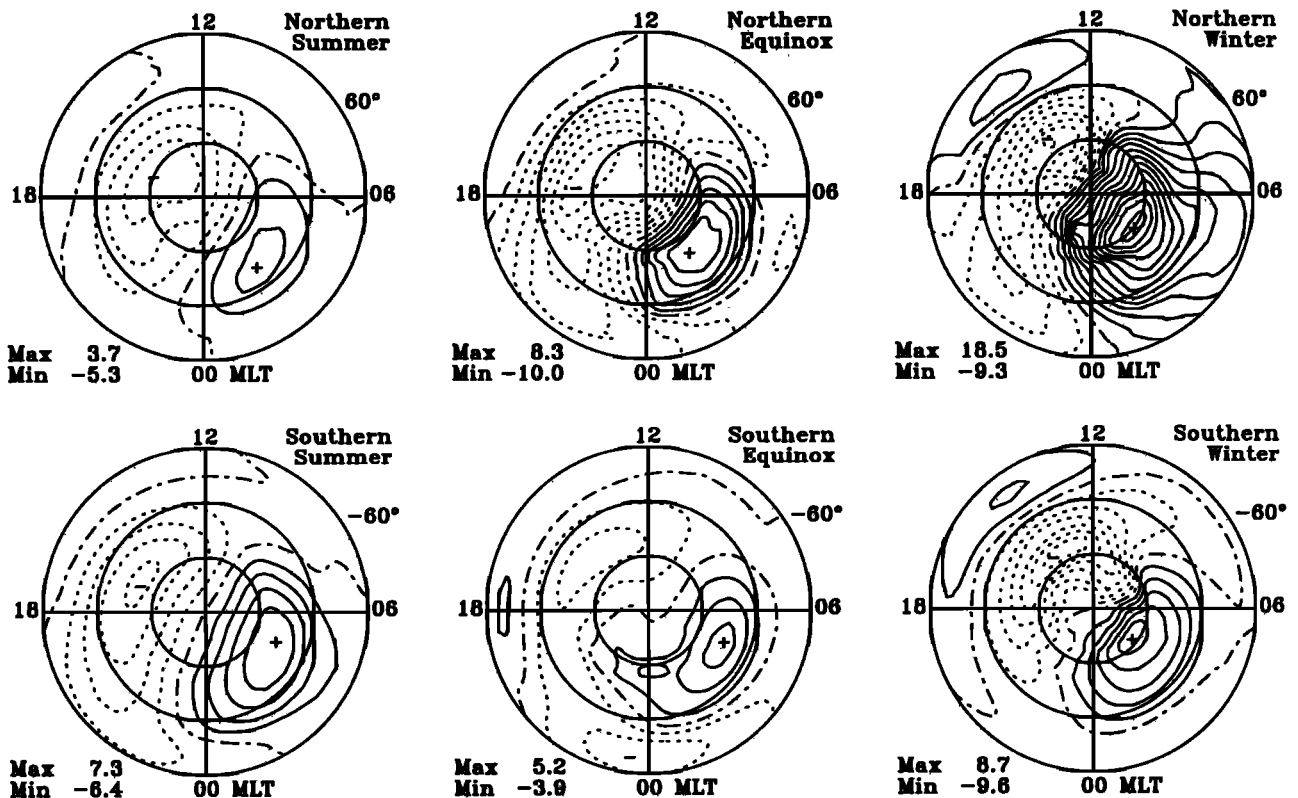


Figure 3. Modeled background (free of the IMF impact) electric potential distributions over the northern and southern polar regions for disturbed ($B_z < 0$) conditions. Polar plots are in the corrected geomagnetic latitude – magnetic local time coordinates. Contour intervals equal 1.5 kV.

Table 1. Amplified Electric Potential in Kilovolts Modeled by the IZMEM to Changes of the Interplanetary Magnetic Field 1-nT Step

Season	Hemisphere	f^*	$B_z = B_y = 0$	$B_z < 0$		$B_z > 0$		$B_y < 0$		$B_y > 0$	
				$\pm B_y$	$B_z < 0$	$B_z > 0$	$B_z < 0$	$B_z > 0$	$B_z < 0$	$B_z > 0$	
Summer	northern	3.2	30.4	14.1	-3.2	5.4	5.4	-5.4	-5.4	-5.4	
	southern	3.0	37.8	10.5	-4.5	-4.8	-5.1	6.0	6.6		
Equinox	northern	2.3	41.4	15.4	-2.5	4.6	4.4	-4.6	-4.4		
	southern	2.7	30.5	13.0	-2.4	-0.5	-0.5	2.7	3.0		
Winter	northern	1.5	40.5	13.0	-4.8	4.8	2.7	-4.8	-2.7		
	southern	2.5	40.5	15.8	-5.8	-4.8	-3.8	7.8	7.0		
Average	potential	drop	36.8 ± 5.1	13.6 ± 1.9	-3.9 ± 1.4		$\pm 3.9 \pm 1.7$		$\pm 5.0 \pm 1.7$		

*Amplification factors f are calculated from the cross-polar background electric potential ~ 35 kV, derived by *Reiff et al.* [1981].

turbed and quiet conditions) values for summer, equinox, and winter are 9.5, 18.0, and 27.1 kV respectively in the northern hemisphere, and 12.6, 11.3, and 16.2 kV in the southern one. The electric potential significantly increases in the northern hemisphere from summer to winter; this is not the case for the southern hemisphere. We have no explanation for this: perhaps it is a natural phenomenon or the northern ionospheric conductivity causes this discrepancy.

If we assume that the viscous cross-polar electric potential is not changing with the season, we can compare the modeled values with the background potential of $\sim 35 \pm 10$ kV obtained by *Reiff et al.* [1981] from the low-altitude satellite observations. Recalling that the IZMEM derives smaller values than actual measurements, we may divide the background potential by the averaged modeled values and then fit the obtained ratios by a straight line against the division of the year into seasons (four months each). This procedure results in the amplification factors: summer 3.2 (north), 3.0 (south); equinox 2.3 (N), 2.7 (S); winter 1.5 (N), 2.5 (S). These numbers can be used for further amplification of modeled (for each IMF parameter) values until more information about ionospheric conductivity in the southern polar region will be collected. Table 1 shows the amplification factors, corresponding modeled background cross-polar potential, and the potential values for different IMF components. Average cross-polar potential of 36.8 kV (after amplification) for the IMF $B_z = B_y = 0$ condition is guaranteed to be close ~ 35 kV derived by *Reiff et al.* [1981].

Modeled Electric Potential for $B_z < 0$

Figure 4 shows the standard two-cell convection patterns caused by the southward IMF ($B_z < 0$), which would be classified as “merging” cells in the model of *Reiff and Burch* [1985]. Modeled patterns are very similar in both hemispheres with antisunward transpolar convection flow which is directed generally from 1000–1100 MLT to 2000–2200 MLT [*Friis-Christensen et al.*, 1985]. This flow moves through the center of polar

caps during summer and equinox; however, it is displaced towards afternoon in winter. During summer both dawn and dusk convection vortices are approximately equal; the dawn cell is larger in both hemispheres during equinox and winter.

The cross-polar (dawn-dusk) potential inferred from IZMEM is slightly larger in the northern hemisphere: summer 4.4 kV (north), 3.5 kV (south); equinox 6.7 kV (N), 4.8 kV (S); winter 8.7 kV (N), 6.3 kV (S). However, amplification of these values by the corresponding factor from Table 1 results in the comparable cross-polar potential. The average cross-polar potential change for a 1-nT step of the southward IMF is 13.6 kV. This is comparable with the value inferred by *Reiff et al.* [1981]: see equation $\Phi(\text{kV}) = 32 \pm 14.7 B_s$ for $B_s < 7$ nT in their Table 1. As these merging convection cells encompass the viscous cells, the total cross-polar potential will increase correspondingly. A typical value of the cross-polar potential for the IMF $B_z = -5$ nT and average solar wind conditions will be around 100 kV in accordance with the numbers from Table 1.

Modeled Electric Potential for $B_z > 0$

Figure 5 shows the ‘reverse’ two-cell convection patterns for the northward IMF ($B_z > 0$), which would be classified as “lobe” cells in the model of *Reiff and Burch* [1985]. The sunward convection flow is directed from midnight to dayside over the near-pole region. The main finding here is that the reverse convection cells are spreading over the entire polar region; they are not limited to the high-latitude polar cap only as suggested by *Reiff and Burch* [1985]. *Friis-Christensen et al.* [1985] have obtained also the expanded reverse convection down to 70° latitude, but their results do not reveal the sunward convection flow near the noon meridian.

The reverse convection in our model extends over auroral latitudes and forms a third convection cell situated near midnight during equinox and winter. The flow concentrates near midnight at $\sim \pm 77^\circ$ latitude during the southern equinox and northern winter. This may

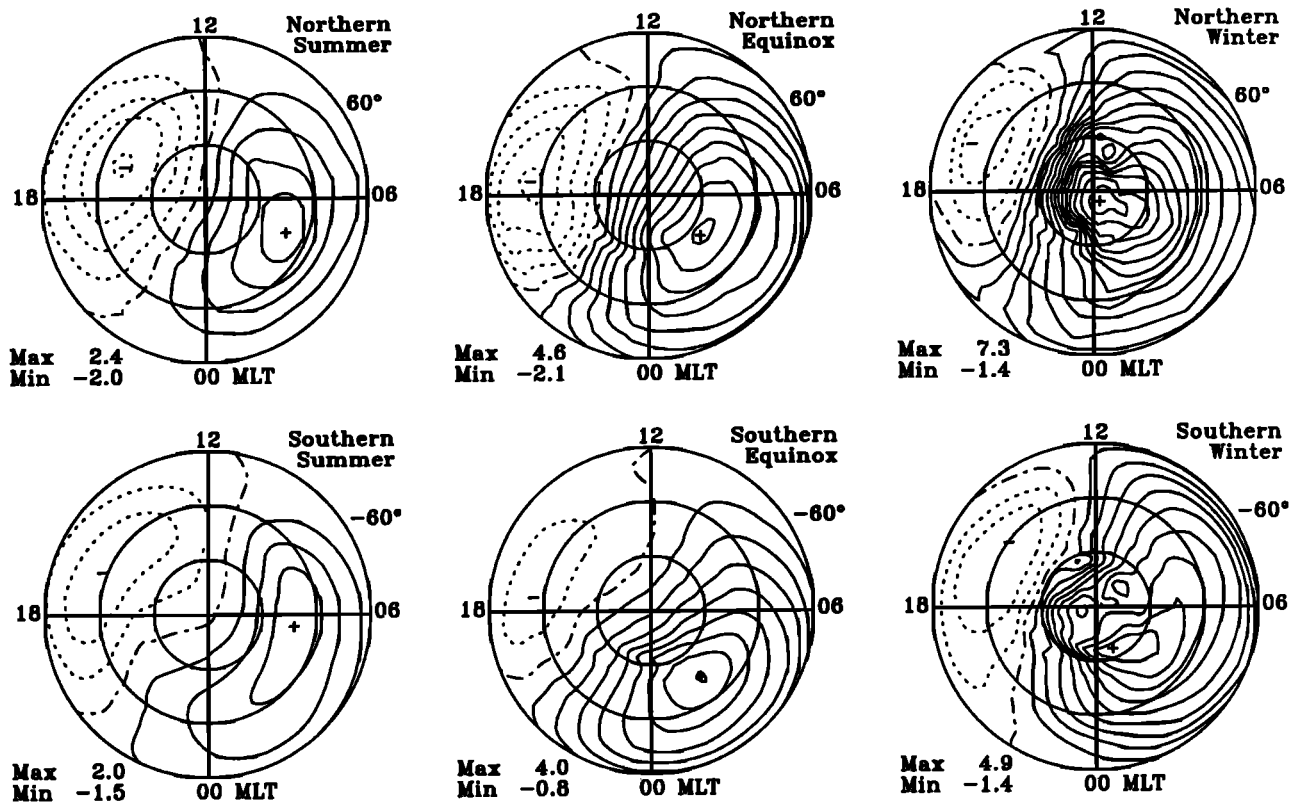


Figure 4. Modeled electric potential distributions for the southward IMF ($B_z = -1$ nT) component. Contour intervals equal 0.5 kV.

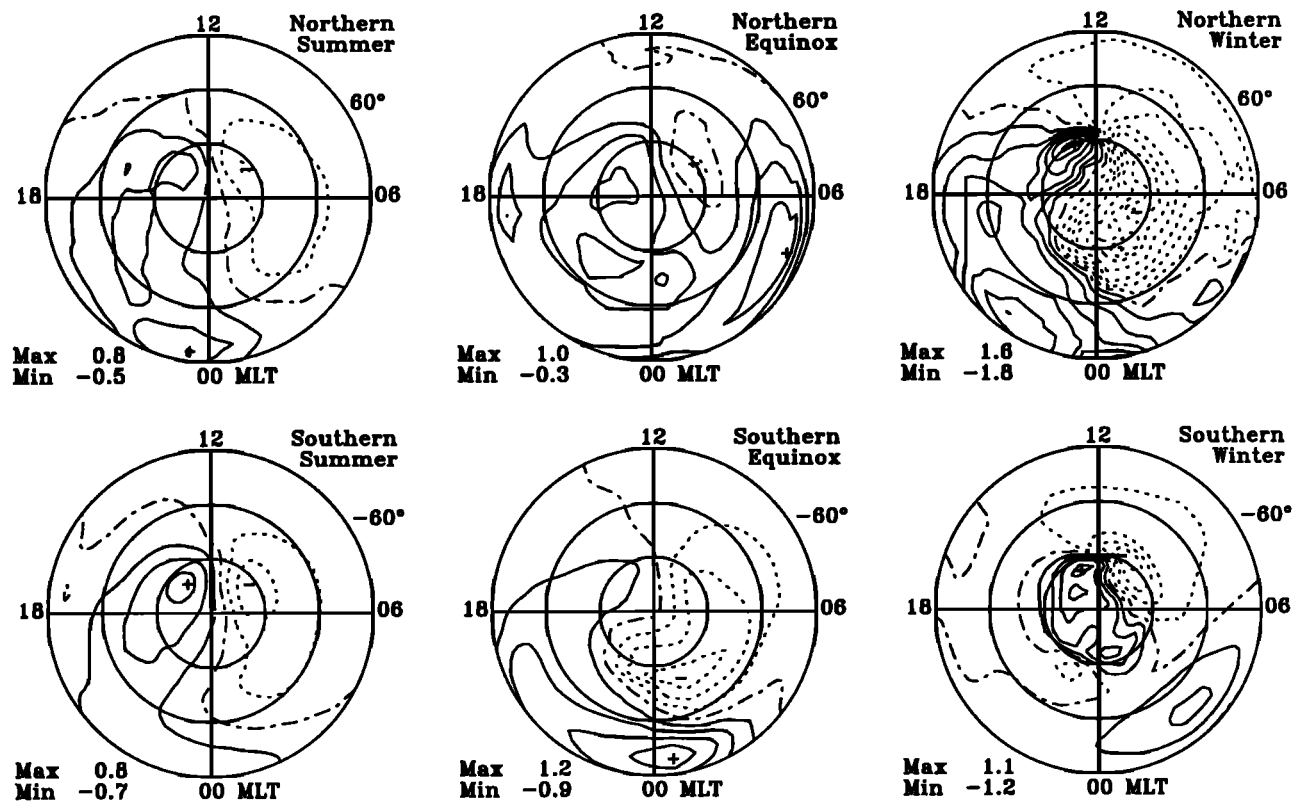


Figure 5. Modeled electric potential distributions for the northward IMF ($B_z = +1$ nT) component. Contour intervals equal 0.25 kV.

be a manifestation of substorms which occurred during northward B_z (note that UT hours with substorm's activity were not excluded from geomagnetic data subjected to regression analyses).

The reverse convection is caused by "dusk-dawn" electric fields. Because the MAX and MIN values on the figure may show extreme points over the entire polar region, the dusk-dawn potential across a dayside portion of the polar cap must be taken into account separately: summer -1.0 kV (north), -1.5 kV (south); equinox -1.1 kV (N), -0.9 kV (S); winter -3.2 kV (N), -2.3 kV (S). Amplification of these values by the corresponding factor from Table 1 results in the comparable potential drops. The average cross-polar potential change for a 1-nT step of the northward IMF is -3.9 kV. There is still a recognizable seasonal asymmetry: the "summer north" potential equals -3.2 kV, and the "winter south" one equals -5.8 kV. The other pair ("summer south" and "winter north") have closer values: -4.5 kV and -4.8 kV. *Reiff et al.* [1981] theorized that they may overestimate the ~ 35 kV background potential drop by as much as 5 kV because of the presence of an embedded reverse convection cell (i.e., $B_z > 0$) in the analyzed data. This value is comparable with our -3.9 kV per $+1$ nT of B_z .

Modeled Electric Potential for B_y

Figures 6 and 7 show the single-cell convection patterns for the IMF azimuthal B_y component during the disturbed ($B_z < 0$) conditions. Similar patterns dur-

ing the quiet ($B_z > 0$) conditions are not shown. This represents the ionospheric current system termed DPY by *Friis-Christensen and Wilhelm* [1975]. The DPY current system is produced by meridional electric fields whose dawn-dusk potential difference is almost zero [*Feldstein and Levitin*, 1986]. Therefore only the electric potential across the polar cusps must be considered for the IZMEM calibration purposes (equatorward ionospheric electric field is assumed as positive).

Convection in both Figures 6 and 7 is in an agreement with the Svalgaard-Mansurov effect, which indicates a different direction of flows in the northern and southern polar caps for the same sign of B_y . The central vortex in the northern hemisphere is well developed during all seasons of the year; its center shifts with a season from magnetic pole to 85° latitude along the 1100 MLT meridian. This movement is more complicated in the southern hemisphere. The northern nightside positive (negative in Figure 7) vortex becomes larger during equinox and winter. The southern potential patterns are more structured. The near-cusp DPY currents are well developed during all seasons except the southern equinox. The nightside "DPY-type" currents concentrate during equinox and winter near $80^\circ - 85^\circ$ in both hemispheres.

The "cross-cusp" potential (Figure 6) inferred from the IZMEM for the IMF positive B_y during the disturbed conditions are summer 1.7 kV (north), -1.6 kV (south), equinox 2.0 kV (N), -0.2 kV (S), winter 3.2 kV (N), -1.9 kV (S). The same values during the quiet

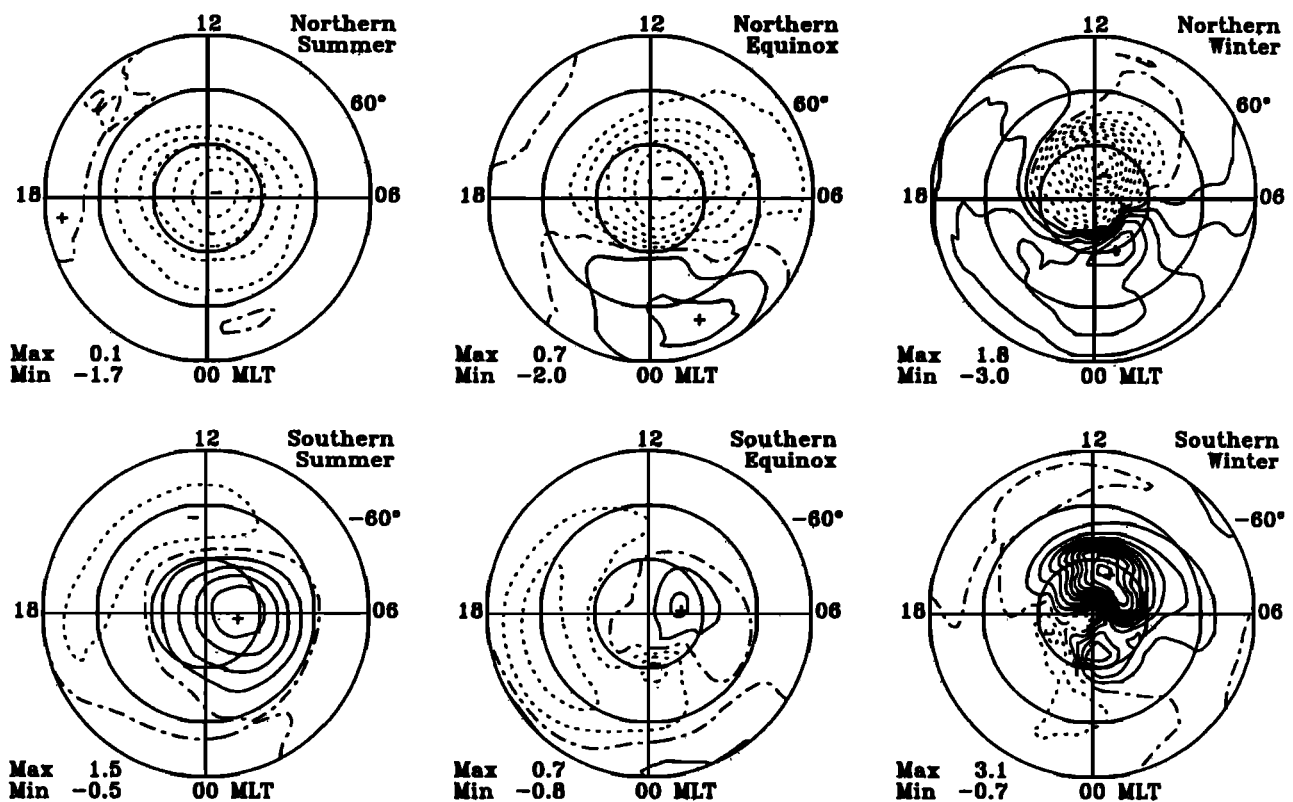


Figure 6. Modeled electric potential distributions during disturbed ($B_z < 0$) conditions for the positive azimuthal IMF ($B_y = +1$ nT) component. Contour intervals equal 0.3 kV.

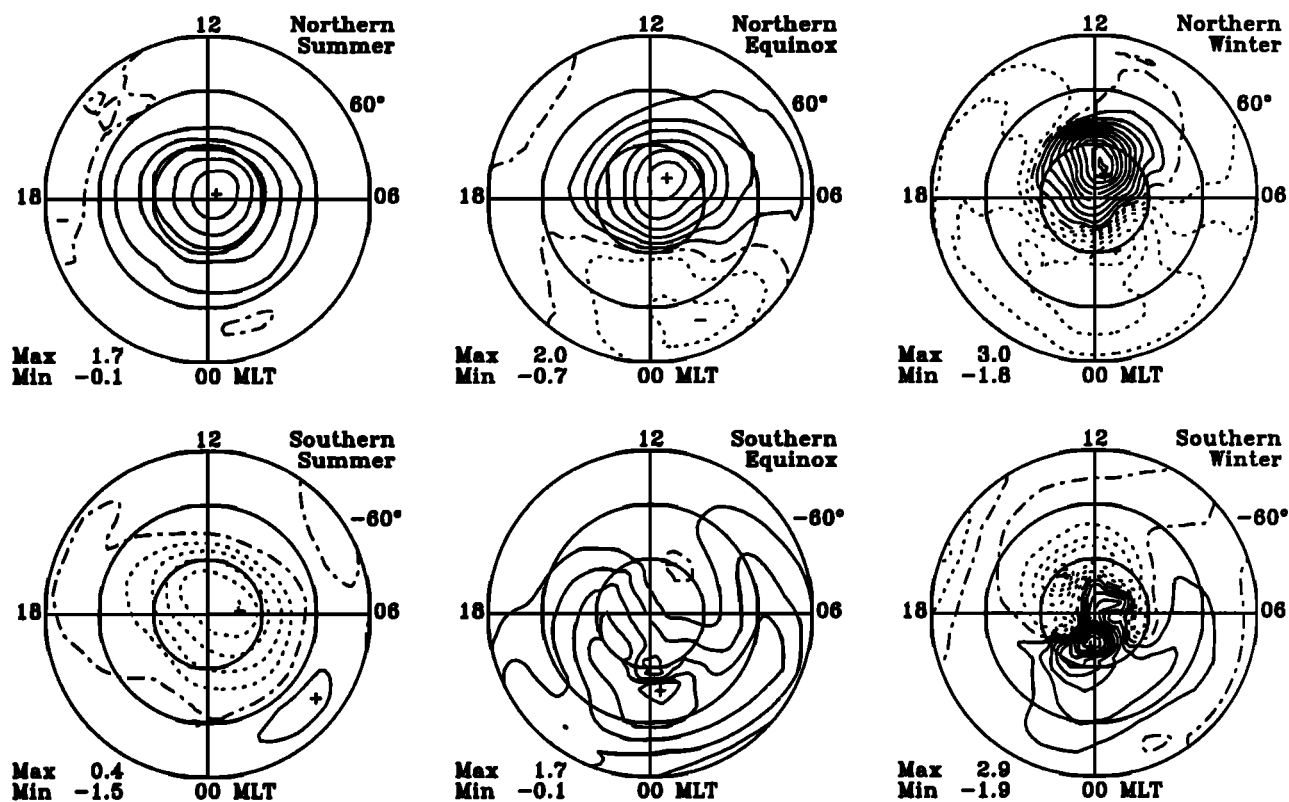


Figure 7. The same electric potential distributions as on Figure 6 but for the negative azimuthal IMF ($B_y = -1$ nT). Contour intervals equal 0.3 kV.

conditions (not shown) are summer 1.7 kV (N), -1.7 kV (S), equinox 1.9 kV (N), -0.2 kV (S), winter 1.8 kV (N), -1.5 kV (S).

The same cross-cusp potential in the northern hemisphere for negative IMF B_y are opposite to that in Figure 6 because the northern geomagnetic data were not separated for the regression analyses by the sign of B_y . The southern cross-cusp potential (Figure 7) for the disturbed conditions are summer 2.0 kV, equinox 1.0 kV, and winter 3.1 kV. Same values for the quiet conditions (not shown) are summer 2.2 kV, equinox 1.1 kV, and winter 2.8 kV. Table 1 presents all these values after amplification.

It seems that a division of the original geomagnetic data according to the IMF disturbed and quiet conditions plays a lesser role than a division in accordance with the IMF B_y sign. The average cross-cusp potential change for a 1-nT step of the IMF B_y component equals ± 5.0 kV for positive B_y , and ± 3.9 kV for negative B_y , that is, the IMF $B_y > 0$ component causes larger geomagnetic disturbances than $B_y < 0$. On the average, the IMF azimuthal component produces ~ 4.5 kV of the cross-cusp potential to changes in 1 nT of B_y .

Discussion

The elementary convection patterns presented in this paper should not be compared directly with existing empirical convection models, for example, the models

of Heppner and Maynard [1987] or Hairston and Heelis [1990]. Each of these elementary convection cells represents a separate component of the IMF interaction with the magnetosphere and its ionospheric manifestation. The final pattern is a superposition of the elementary cells for any given situation in the IMF. Heppner and Maynard [1987] stated that standard two-cell convection pattern can be rotationally twisted clockwise when the IMF B_z becomes strong, and the sign and magnitude of B_y will play a significant role in the distortion. Their model shows a sunward convection in the dayside polar cap as a deformation of the two-cell pattern. After a massive analysis of satellite data the authors concluded that "...the nightside dilemmas that plague three- and four-cell models designed to explain sunward convection in polar regions under $+B_z$ conditions do not appear..." [Heppner and Maynard, 1987, p. 4467]. A similar conclusion: "...the clockwise rotation of the potential pattern with increasing B_z (positive) while the conductivity remains constant..." was made by Feldstein and Levitin [1986, p. 1170] from the analysis of ground-based geomagnetic data only. The results presented here confirm these conclusions.

The asymmetry in geometry of convection patterns in both hemispheres may be caused by an application of the northern ionospheric conductivity model, and perhaps also by a natural "north-south" asymmetry in the electric potential. The southern geomagnetic pole, for example, is located asymmetrically against the northern one; southern polar magnetic local midnight occurs

at 1530 UT – only 10 hours past the local midnight at the north geomagnetic pole at 0530 UT. Ellipticity of the Earth's orbit may also enhance the asymmetry of the polar cap potential distributions because the planet is in its perihelion in the beginning of January and the southern polar cap is lighted better. Therefore the ionospheric conductivity should be slightly larger for "summer australis" than for "summer borealis". The latter is not applicable for equinoctial months and for winters in both hemispheres. For example, we found the "northern background" potential smaller during summer than the "southern background" one (30.4 kV and 37.8 kV respectively; see Table 1), but both potentials are equal during winter. One can see from equation (3) that the southern summer potential should be larger if the smaller (due to the influence of the Earth's orbit ellipticity) northern summer ionospheric conductivity is applied to the southern hemisphere. The relative perihelion–aphelion difference in the Sun–Earth distance is about 3 %, which means that the corresponding illumination (and hence conductivity) of polar ionospheres should differ by about 6%.

The IZMEM can successfully model magnetic and electric fields measured by satellites, for example, Cosmos 184 [Belov *et al.*, 1984], Magsat [Dremukhina *et al.*, 1985], OGO 6 [Feldstein and Levitin, 1986], DE 2 [Dremukhina *et al.*, 1990]. It was found that the IZMEM output values are smaller, in general, than measurements by factor $\sim 3.0 - 3.5$. Similar values are obtained for the summer season in this paper and the corresponding amplification factors are estimated for equinox and winter. These numbers should be confirmed or corrected in future studies.

In conclusion, we summarize average values of electric potential caused by 1-nT step in the IMF as they are modeled by IZMEM with the use of amplification factors: ~ 14 kV for the IMF southward B_z , ~ -4 kV for the IMF northward B_z , and $\sim \pm 4.5$ kV for the IMF azimuthal B_y components. The average background cross-polar potential for the zero IMF is ~ 37 kV. A combination of the elementary cells allows one to model quantitatively the convection patterns for different conditions in the IMF. For example, a combination of the viscous and merging cells for $B_z = -5$ nT gives 107 kV of the dawn-dusk potential drop. This value may change drastically for strong B_y . The background potential will be eroded during positive B_z , but it will not become zero for $B_z = 7$ nT because the corresponding electric field develops in the dayside polar cap only. Large reverse cross-polar potential ~ 80 kV may develop for $B_z = +10$ nT and $B_y = \pm 10$ nT.

The IZMEM model can be used to investigate the particular case studies but it is limited to specifying large-scale, quasi-steady events. While it works fine for hourly mean values, it can also be used for studying time-varying phenomena; in that case a proper time delay between the IMF changes and their manifestation on the Earth's surface should be taken into account. The "geomagnetic activity history" during last 20–40 min is also important, for example, if a substorm occurs

during this period, the model can not be applied. The latter conclusion is not firm in all cases and we continue to investigate capabilities of the IZMEM to model such short-term events.

Finally, the IZMEM model may be used in comparison with the results of other modeling techniques. For example, the AMIE technique uses an initial distribution of electric potential, then ground-based geomagnetic data and additional satellite and radar measurements are subjected to the analysis. We believe that AMIE technique will provide a good output if a good ground-based coverage is achieved. However, Arctic ocean and Antarctic large land mass will never be properly covered with geomagnetic observations. So, there is a problem of getting good global coverage for AMIE modeling. The IZMEM model can provide an initial estimation of global potential distributions as a valuable input for the AMIE technique at least when the IMF data are available. The IZMEM model may analyze particular events when the ground-based geomagnetic data collection is impossible or significantly delayed.

The IZMEM model has also a "now-casting" capability providing realistic convection patterns over the entire polar regions. Since there are low-altitude satellite plasma drift measurements (e.g., DMSP data), the electric potential inferred from these data can be compared with a set of modeled cross-polar potential profiles along satellite trajectories, which may represent a number of situations in the IMF; for example, electric potential patterns can be modeled in advance for each 1-nT step between -30 to $+30$ nT of B_z and B_y . The modeled profile similar to the observed data gives an approximate estimation of the IMF values during the satellite pass, and, therefore, the IZMEM can reproduce (now-cast) the entire convection patterns over both polar regions. Another example is that if the IMF data will be available an hour in advance (e.g., from the L1 satellite), the IZMEM can predict the potential pattern configuration and magnitude in both polar regions. The IZMEM exhibits these capabilities for the large-scale, quasi-steady events, but the model cannot forecast magnetic substorm.

Acknowledgments. We would like to thank Robert Clauer for valuable comments, discussion, and help with preparation of the paper. Marie Cooper has provided assistance in programming on IDL. This work has been supported by the Russian Foundation for Fundamental Research under the grant 93-05-8722. One of the authors (V.O.P.) has been supported by the University of Michigan under funding from the National Science Foundation grant ATM-9106958. V.O.P. especially thanks both referees for their assistance in the evaluation of the paper's clarity and language.

The Editor thanks two referees for their assistance in evaluating this paper.

References

- Afonina, R. G., B. A. Belov, A. E. Levitin, M. Yu. Markova, Ya. I. Feldstein, and M. V. Fiskina, Connection of components of the interplanetary magnetic field with field-

- aligned currents in high-latitudes of the northern hemisphere, *Geomagn. Aeron.*, **20**, 1073, 1980.
- Alcayde, D., G. Gaudal, and J. Fontanari, Convection electric fields and electrostatic potential over $61^\circ < \Lambda < 71^\circ$ invariant latitude results, *J. Geophys. Res.*, **91**, 233, 1986.
- de la Beaujardiere, O., D. Alcayde, J. Fontanari, and C. Leger, Seasonal dependence of high-latitude electric fields, *J. Geophys. Res.*, **96**, 5723, 1991.
- Belov, B. A., R. G. Afonina, A. E. Levitin, and Ya. I. Feldstein, The effects of interplanetary magnetic field orientation on geomagnetic field at the northern polar cap (in Russian), in *Variations of Magnetic Field and the Aurora*, edited by Ya. I. Feldstein and A. E. Levitin, p. 15, IZMIRAN, Moscow, 1977.
- Belov, B. A., Yu. I. Galperin, L. V. Zinin, A. E. Levitin, R. G. Afonina, and Ya. I. Feldstein, Plasma convection in the polar ionosphere: A comparison of the satellite Cosmos-184 measurements and the model related to the IMF vector, *Kosm. Issled.*, **22**, 201, 1984.
- Blomberg, L. G., and G. T. Marklund, High-latitude convection patterns for various large-scale field-aligned current configurations, *Geophys. Res. Lett.*, **18**, 717, 1991.
- Clauer, C. R., The technique of linear prediction filters applied to studies of solar wind-magnetosphere coupling, in *Solar Wind-Magnetosphere Coupling*, edited by Y. Kamide and J. A. Slavin, p. 39, Terra Scientific, Tokyo, 1986.
- Clauer, C. R., and E. Friis-Christensen, High-latitude day-side electric fields and currents during strong northward interplanetary magnetic field: Observations and model simulation, *J. Geophys. Res.*, **93**, 2749, 1988.
- Dremukhina, L. A., Ya. I. Feldstein, and A. E. Levitin, Model calculations of currents and magnetic fields along a Magsat trajectory, *J. Geophys. Res.*, **90**, 6657, 1985.
- Dremukhina, L. A., A. E. Levitin, and Ya. I. Feldstein, Convection in high latitudes in periods $B_z > 0$, *Geomagn. Aeron.*, Engl. Transl., **30**, 160, 1990.
- Faermark, D. S., A restoration of 3-dimensional current systems in high-latitudes by the use of ground-based geomagnetic observations, *Geomagn. Aeron.*, Engl. Transl., **17**, 114, 1977.
- Feldstein, Ya. I., A. E. Levitin, D. S. Faermark, R. G. Afonina, B. A. Belov, and V. Yu. Gaidukov, Electric fields and potentials in the high-latitude ionosphere for different situations in the interplanetary space, *Planet. Space Sci.*, **32**, 907, 1984.
- Feldstein, Ya. I., and A. E. Levitin, Solar wind control of electric fields and currents in the ionosphere, *J. Geomagn. Geoelectr.*, **38**, 1143, 1986.
- Foster, J. C., An empirical electric field model derived from Chatanika radar data, *J. Geophys. Res.*, **88**, 981, 1983.
- Friis-Christensen, E., and J. Wilhjelm, Polar cap currents for different directions of the interplanetary magnetic field in the $Y-Z$ plane, *J. Geophys. Res.*, **80**, 1248, 1975.
- Friis-Christensen, E., Y. Kamide, A. D. Richmond, and S. Matsushita, Interplanetary magnetic field control of high-latitude electric field and currents determined from Greenland magnetometer data, *J. Geophys. Res.*, **90**, 1325, 1985.
- Hairston, M. R., and R. A. Heelis, Model of high-latitude ionospheric convection pattern during southward interplanetary magnetic field using DE 2 data, *J. Geophys. Res.*, **95**, 2333, 1990.
- Heelis, R. A., J. K. Lowell, and R. W. Spiro, A model of the high-latitude ionospheric convection pattern, *J. Geophys. Res.*, **87**, 6339, 1982.
- Heppner, J. P., Polar cap electric field directions related to the interplanetary magnetic field direction, *J. Geophys. Res.*, **77**, 4877, 1972.
- Heppner, J. P., Empirical models of high-latitude electric fields, *J. Geophys. Res.*, **82**, 1115, 1977.
- Heppner, J. P., and N. C. Maynard, Empirical high-latitude electric field models, *J. Geophys. Res.*, **92**, 4467, 1987.
- Kamide, Y., A. D. Richmond, and S. Matsushita, Estimation of ionospheric electric fields, ionospheric currents and field-aligned currents from ground magnetic records, *J. Geophys. Res.*, **86**, 801, 1981.
- Kern, J. W., Analysis of polar magnetic storms, *J. Geomagn. Geoelectr.*, **18**, 125, 1966.
- Knipp, D. J., A. D. Richmond, B. Emery, N. U. Crooker, O. de la Beaujardiere, D. Evans, and H. Kroehl, Ionosphere convection response to changing IMF direction, *Geophys. Res. Lett.*, **18**, 721, 1991.
- Knipp, D. J., et al., Ionospheric convection response to slow, strong variations in a northward interplanetary magnetic field: A case study for January 14, 1988, *J. Geophys. Res.*, **98**, 19273, 1993.
- Levitin, A. E., R. G. Afonina, B. A. Belov, and Ya. I. Feldstein, Geomagnetic variations and field-aligned currents at northern high-latitudes and their relations to solar wind parameters, *Phil. Trans. R. Soc. London Ser. A*, **304**, 253, 1982.
- Maezawa, K., Magnetospheric convection induced by the interplanetary magnetic field: Quantitative analysis using polar cap magnetic records, *J. Geophys. Res.*, **81**, 2289, 1976.
- Mansurov, S. M., O. A. Troshichev, A. N. Zaitzev, V. O. Papitashvili, G. A. Timofeev, and M. A. Kandibolotskaya, Characteristics of magnetic disturbances produced by the IMF in the southern polar cap, *Geomagn. Aeron.*, Engl. Transl., **21**, 428, 1981.
- Mishin, V. M., M. I. Matveev, G. B. Shpynev, A. D. Bazarzhapov, and V. K. Kompanets, Preliminary results of the three-dimensional current system calculations from the ground-based geomagnetic disturbances (in Russian), *Issled. Geomagn. Aeron. Fiz. Solntsa*, **43**, 14, 1977.
- Mishin, V. M., A. D. Bazarzhapov, and G. B. Shpynev, Electric fields and currents in the Earth's magnetosphere, in: *Dynamics of the Magnetosphere*, edited by S.-I. Akasofu, pp. 249-268, D. Reidel, Norwell, Mass., 1980.
- Papitashvili, V. O., Relationship between geomagnetic variations in the polar cap and the interplanetary magnetic field during the solar activity cycle, *Geomagn. Aeron.*, Engl. Transl., **22**, 130, 1982.
- Papitashvili, V. O., and C. R. Clauer, Comparison and calibration of the modeled high-latitude convection patterns with observations from the January 27-29, 1992 GEM campaign, *Eos Trans. AGU*, **74**, 254, 1993.
- Papitashvili, V. O., O. A. Troshichev, and A. N. Zaitzev, Linear dependence of the intensity of geomagnetic variations in the polar region on the magnitudes of the southern and northern components of the interplanetary magnetic field, *Geomagn. Aeron.*, Engl. Transl., **21**, 565, 1981.
- Papitashvili, V. O., A. N. Zaitzev, and Ya. I. Feldstein, Magnetic disturbances generated by the interplanetary magnetic field in the southern polar cap during the summer, *Geomagn. Aeron.*, Engl. Transl., **23**, 506, 1983.
- Papitashvili, V. O., B. A. Belov, and L. I. Gromova, Field-aligned currents and convection patterns in the southern polar cap during stable northward, southward, and azimuthal IMF, *IEEE Trans. Plasma Sci.*, **17**, 167, 1989.
- Papitashvili, V. O., Ya. I. Feldstein, A. E. Levitin, B. A. Belov, L. I. Gromova, and T. E. Valchuk, Equivalent ionospheric currents above Antarctica during the austral summer, *Antarct. Sci.*, **2**, 67, 1990.
- Papitashvili, V. O., B. A. Belov, Ya. I. Feldstein, S. A. Golyshev, L. I. Gromova, and A. E. Levitin, Model of relations between the solar wind and IMF parameters and

- geomagnetic variations at high-latitudes, in *Proceedings of Solar-Terr. Predict. IV Workshop, Ottawa, Canada, May 18-22, 1992*, vol. 3, edited by J. Hruska, M. A. Shea, D. F. Smart, and G. Heckman, p. 229, National Oceanic and Atmospheric Administration, Boulder, Colo., 1993.
- Reiff, P. H., and J. L. Burch, IMF B_y -dependent plasma flow and Birkeland currents in the dayside magnetosphere, 2, A global model for northward and southward IMF, *J. Geophys. Res.*, **90**, 1595, 1985.
- Reiff, P. H., R. W. Spiro, and T. W. Hill, Dependence of polar cap potential drop on interplanetary parameters, *J. Geophys. Res.*, **86**, 7639, 1981.
- Richmond, A. D., and Y. Kamide, Mapping electrodynamic features of the high-latitude ionosphere from localized observations: Technique, *J. Geophys. Res.*, **93**, 5741, 1988.
- Robinson, R. M., and R. R. Vondrak, Measurement of E region ionization and conductivity produced by solar illumination at high latitudes, *J. Geophys. Res.*, **89**, 3951, 1984.
- Troshichev, O. A., Polar magnetic disturbances and field-aligned currents, *Space Sci. Rev.*, **32**, 275, 1982.
- Wallis, D. D., and E. E. Budzinski, Empirical models of height-integrated conductivities, *J. Geophys. Res.*, **86**, 125, 1981.
-
- V. O. Papitashvili, B. A. Belov, D. S. Faermark, Ya. I. Feldstein, S. A. Golyshchev, L. I. Gromova, and A. E. Levitin, IZMIRAN, Troitsk, Moscow Region, 142092, Russia.

(Received August 24, 1993; revised March 21, 1994; accepted March 23, 1994.)